Chinese Chemical Letters 33 (2022) 2517–2521

Contents lists available at ScienceDirect

Chinese Chemical Letters

journal homepage: www.elsevier.com/locate/cclet

Tetrahedral framework nucleic acids regulate osteogenic differentiation potential of osteoporotic adipose-derived stem cells

Tianyu Chen[a], Dexuan Xiao[a], Yanjing Li[a], Sirong Shi[a], Xiao Yang[a], Shuanglin Peng[a], Bin Guo[b,*], Xiaoxiao Cai[a,*]

[a] State Key Laboratory of Oral Diseases, National Clinical Research Center for Oral Diseases, West China Hospital of Stomatology, Sichuan University, Chengdu 610041, China
[b] Department of Stomatology, First Medical Center of Chinese PLA General Hospital, Beijing 100853, China

ARTICLE INFO

Article history:
Received 29 September 2021
Revised 26 November 2021
Accepted 30 November 2021
Available online 4 December 2021

Keywords:
Osteoporosis
Tetrahedral framework nucleic acid
Adipose-derived stem cell
Autologous stem-cell transplantation
Osteogenic differentiation

ABSTRACT

Osteoporosis (OP) is a noncommunicable bone disease caused by a shift in the balance between osteoblasts and osteoclasts, and can severely affect the health of elderly persons. Autologous stem-cell transplantation can improve reduced bone density and weakened fracture healing abilities in patients with OP. However, OP can adversely affect the osteogenesis and proliferation abilities of autologous adipose-derived stem cells (ASCs). Therefore, an effective drug is required to facilitate autologous ASCs to recover their osteogenic and proliferative potential. Tetrahedral framework nucleic acid (tFNA) is a new type of nanomaterial that has ability to regulate the biological behavior of cells effectively and enhance the bioactivity of stem cells. In this study, we examine the effects of tFNAs on the osteogenic differentiation and proliferation abilities of ASCs in rats with OP. The results indicate that the 250 nmol/L tFNAs can considerably increase the expression of osteogenesis-related markers, effectively promote the proliferation and osteogenic differentiation of osteoporotic ASCs (OP-ASCs), and help them to regain their osteogenic and proliferative potential. In short, tFNAs can enable OP-ACSs to recover their osteogenic potential and promote their proliferation and, therefore, can play a key regulatory role in autologous ASC transplantation.

Osteoporosis (OP) is a major bone disease that often occurs in postmenopausal women. Its onset is characterized by bone loss and deterioration of the bone tissue microstructure [1,2]. Hip fractures caused by OP can lead to a decreased quality of life, increased risk of death, and the inability to live independently [3,4]. Therefore, OP is recognized as an important health problem by the World Health Organization [5]. The existing treatment for OP relies mainly on drugs that focus on increasing bone mass and bone density [6–8]. In addition, some new nanomaterials can also have a certain effect on bone regeneration. However, these treatments are limited by the adverse effects of the drugs and the uncertainty of long-term efficacy [9,10]. In the patients with OP, the decrease in bone density and fracture healing ability may be related to the reduced osteoblast differentiation and proliferation that is caused by the lack of mesenchymal stem cells [11], therefore ASC transplantation is a promising treatment for OP.

According to previous studies, the osteogenic potential of an adipose-derived stem cell (ASC) is similar to that of a bone marrow-derived stem cell, but with the advantages of high yield, easy cultivation, and faster growth rates [12]. Therefore, for patients with OP, autologous transplantation of ASCs promises higher safety and feasibility. However, a recent study demonstrated that, compared with normal mice, the proliferation and osteoblast differentiation of ASCs in mice suffering from OP are greatly reduced [13], which presents challenges in autologous ASC transplantation treatment. A drug that can effectively restore the proliferation and osteoblast differentiation of OP-ASCs is therefore necessary to ensure the effectiveness of the treatment.

The tFNA is composed of four single-stranded DNA in a pyramid-shaped nanostructure [14]. The tFNAs can promote cell proliferation and regulate stem cell differentiation. As it can regulate cell biological behavior, it is an excellent synergist for stem cells [14–16]. Previous studies have shown that tFNAs play a positive role in the treatment of osteoarthritis, and can also regulate the osteoblast differentiation of mesenchymal stem cells through the Wnt/β-catenin pathway [17]. Therefore, we speculate that tF-

* Corresponding authors.
E-mail addresses: guobin0408@126.com (B. Guo), xcai@scu.edu.cn (X. Cai).

https://doi.org/10.1016/j.cclet.2021.11.090
1001-8417/

Table 1
Sequences of ssDNA.

ssDNA	Direction	Base sequence
S1	5′→3′	ATTTATCACCCGCCATAGTAGACGTATCACCAGGCAGTTGAGAC-GAACATTCCTAAGTCTGAA
S2	5′→3′	ACATGCGAGGGTCCAATACCGACGATTACAGCTTGCTACACGAT-TCAGACTTAGGAATGTTCG
S3	5′→3′	ACTACTATGGCGGGTGATAAAACGTGTAGCAAGCTGTAATCGAC-GGGAAGAGCATGCCCATCC
S4	5′→3′	ACGGTATTGGACCCTCGCATGACTCAACTGCCTGGTGATACGAG-GATGGGCATGCTCTTCCCG

Table 2
Sequence of forward and reverse primers of selected genes designed for qPCR.

mRNA		Primer pair
RUNX2	forward	AGGGACTATGGCGTCAAACA
	reverse	GGCTCACGTCGCTCATCTT
OPN	forward	CACTCCAATCGTCCCTACA
	reverse	CTTAGACTCACCGCTCTTCAT
OCN	forward	GGACCCTCTCTCTGCTCACTCTG
	reverse	ACCTTACTGCCCTCCTGCTTGG
ALP	forward	GGCGTCCATGAGCAGAACTACATC
	reverse	CAGGCACAGTGGTCAAGGTTGG
GAPDH	forward	ACAGCAACAGGGTGGTGGAC
	reverse	TTTGAGGGTGCAGCGAACTT

NAs may improve the proliferation and osteoblast differentiation of OP-ASCs, and play a key regulatory role in OP-treated autologous stem cell transplantation

The sequences of the four single strands are shown in Table 1. According to the previous articles published by our laboratory [18], the four single strands are dissolved in Tm buffer (10 mmol/L Tris-HCl, 50 mmol/L $MgCl_2{\cdot}6H_2O$, pH 8.0), heated to 95 °C for 10 min, and cooled to 4 °C for 20 min to obtain tFNAs.

In order to verify the successful synthesis of tFNAs, we applied five methods. According to the previous description, polyacrylamide gel electrophoresis (PAGE) and high performance capillary electrophoresis (HPCE) detected the relative molecular weight of tFNAs and four single chains, transmission electron microscopy (TEM) and atomic force microscopy (AFM) detected the spatial structure and shape of tFNAs, dynamic light scattering (DLS) detected the particle size and potential of tFNAs [19,20].

Animal experiments were approved by the China Committee for Research and Animal Ethics, in compliance with the laws on experimental animals. Thirty 8-week-old female Sprague Dawley rats were stochastic divided into two groups in equal numbers: ovariectomy group (OVX group) and control group. Rats in OVX group were intraperitoneally anesthetized with 1% pentobarbital (40 mg/kg). After the anesthesia took effect, a 5 cm linear incision was made at a position 0.5 cm from the spine and 1 cm below the ribs, then remove the both ovaries through this incision. After removing both ovaries, suture incision of rats. The same procedure was performed on animals in the control group, but the ovaries were not removed. Six weeks after the operation, 6 rats in each of the OVX group and the sham operation group were selected, and the femur metaphysis of the rats was scanned by Micro Computed Tomography (Micro-CT). Microstructural parameters include structure model index (SMI), trabecular separation/spacing (Tb.Sp) and trabecular number (Tb.N).

We extracted ASCs and OP-ASCs from the inguinal fat of 14-week-old female Sprague-Dawley rats and OVX rats, respectively. After finely excising the adipose tissue, it was incubated in 0.075% type I collagenase and incubated for 30 min. Next, the extracted cells were cultured in a 25 cm^2 culture flask using α-MEM medium with 10% fetal bovine serum and 1% penicillin/streptomycin. Extracted cells were cultured in an incubator at 37 °C and 5% CO_2.

To explore the cellular uptake of tFNAs, one of the four single chains was labeled with Cy5, and tFNAs-Cy5 was synthesized according to the aforementioned method [21]. The tFNAs-Cy5 with a concentration of 250 nmol/L was supplied to the OP-ASCs' medium to make the cells take up tFNAs-Cy5 for 24 h. A part of the cells were harvested, rinse and resuspend the cells with phosphate buffered saline (PBS), then the fluorescence intensity of Cy5 in cells was detected by a flow-cytometer. For the remaining cells, the nucleus and cytoskeleton were stained with DAPI and phalloidin respectively, and the Cy5 fluorescence intensity in the cells was observed by confocal microscope.

To test whether tFNAs can promote stem cell viability, OP-ASCs treated with tFNAs at different concentrations (0, 62.5, 125, 250 nmol/L) for 24 h were used to test cell viability through the cell counting kit-8 (CCK-8) (KeyGen-BioTECH, Nanjing, China). Add the working concentration of CCK-8 solution to OP-ASCs treated with different concentrations of tFNAs, incubate at 37 °C for 45 min, and detect the absorbance of the sample at a wavelength of 450 nm in a microplate reader. The migration of OP-ASCs and ASCs under different treatments was evaluated by the *in vitro* scratch wound healing migration assay. Inoculate ASCs and OP-ASCs in a 6-well plate. When the inoculated cells reach 80%−90% confluence, use a sterile pipette tip to produce two intersecting linear scratches. The 6-well plates were then divided into three groups: (1) tFNAs group (OP-ASCs treated with 250 nmol/L tFNAs), (2) OP-ASCs group (OP-ASCs without tFNAs), and (3) ASCs group (ASCs without tFNAs). The three groups of cells obtain wound healing images 24 h after the scratch

OP-ASCs and ASCs were inoculated on a 12-well plate at 1×10^5 cell/cm^5 for osteogenic induction, and divide the 12-well plate into tFNAs group, OP-ASCs group and ASCs group according to the method described earlier, the medium is osteoinduction medium (Cyagen, Guangzhou, China). Seven days after osteogenic induction, alkaline phosphatase was detected with alkaline phosphatase staining kit (KeyGen-BioTECH, Nanjing, China). The steps of alkaline phosphatase staining were as follows: Discard the original medium, and rinse each group of cells with PBS. Cells were fixed with 4% paraformaldehyde at 4 °C for 30 min and then rinsed 3 times with PBS, and incubated with alkaline phosphatase staining buffer at 37 °C for 1 h. Finally, observe and take pictures under an inverted microscope. Alizarin red staining is performed 21 days after osteogenic induction, rinse each group of cells with PBS, fix with 4% paraformaldehyde at 4 °C for 30 min, then rinse 3 times with PBS, incubate with 0.1% Alizarin Red at 37 °C for 30 min. Finally use an inverted microscope to observe the osteogenic differentiation.

In order to detect the expression of OPN, RUNX2 and OCN genes, cells in the OP-ASCs group, tFNAs group and ASCs group were cultured at 37 °C for 21 days. The total mRNA was extracted by trizol (Invitrogen, MA, USA), then mRNA was reverse transcribed into cDNA with a reverse transcription kit (Takara, Dalian, China), the cDNA is quantified by Quantitative Real-Time PCR (q-PCR) using PrimeScript RT-PCR kit (Takara, Dalian, China) according to the previous procedure [22]. The primer sequence of each gene is shown in Table 2.

In order to detect the expression of RUNX2 (runt-related transcription factor 2), OPN (osteopontin), OCN (osteocalcin), ALP (alkaline phosphatase) protein in the cells, the cells were divided into 3 groups according to the previous grouping method, and they were sown into confocal dishes and cultured for 21 days (explore the expression of ALP protein only need culture for 7 days). The cells were perforated according to the method described in the previous article and the antibody was bound to the target protein [23], and then the fluorescently labeled secondary antibody was used to bind the previous antibody, the nucleus and cytoskele-

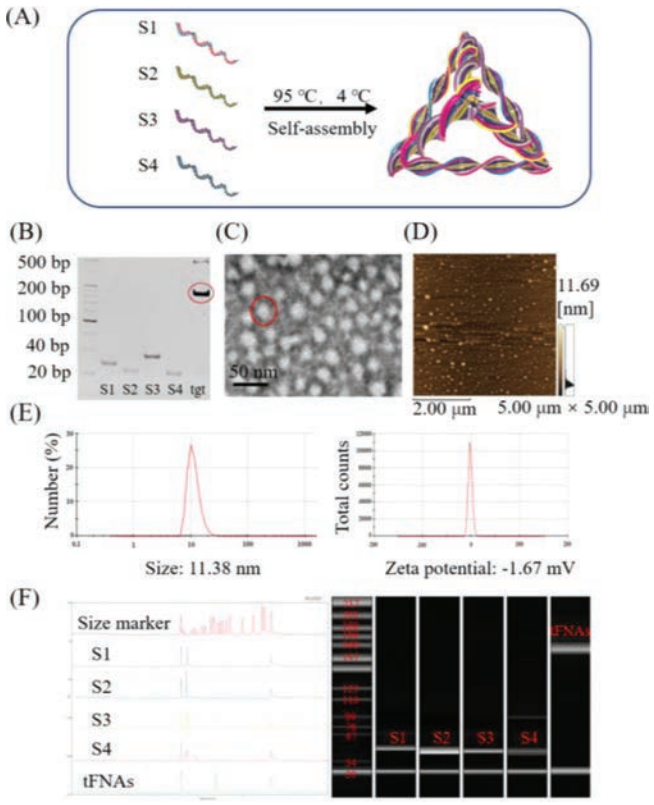

Fig. 1. Successful synthesis and characterization of tFNAs. (A) Diagrammatic sketch of tFNAs. (B) Analysis by 8% PAGE. (C) TEM image of tFNAs. (D) AFM image of tFNAs. (E) Molecular weight of tFNAs detected by HPEC. (F) Hydrodynamic size and zeta potential of tFNAs measured by DLS.

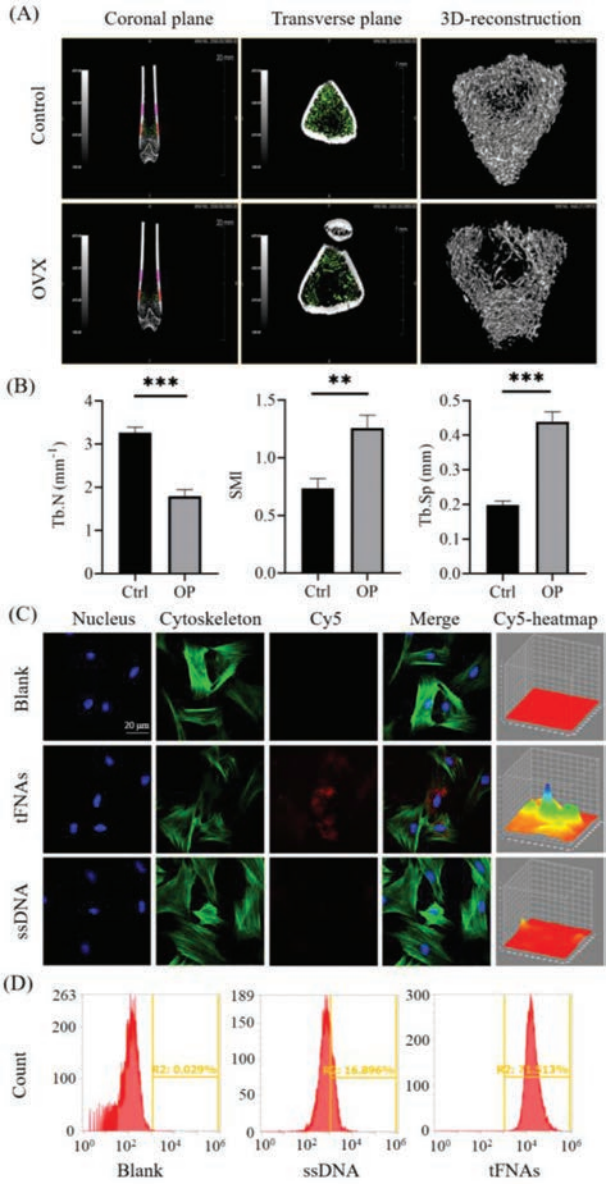

Fig. 2. Establishment a rat model of osteoporosis and cellular uptake of tFNAs ($n = 3$, $^{**}P < 0.01$, and $^{***}P < 0.001$). (A) Micro-CT analysis of the femur metaphysis. (B) Comparison of morphological parameters of the femur metaphysis between the control group and OVX group. (C) Intracellular uptake of tFNAs by a confocal laser microscope (nucleus: blue; cytoskeleton: green; and Cy5: red). Scale bars are 20 μm. (D) Flow cytometry analysis of the proportion of the OP-ASCs uptake of tFNAs.

ton were stained with DAPI and phalloidin, respectively, and the fluorescent expression of the target protein was detected with a confocal laser microscope. In addition to immunofluorescence, we also used western blotting to explore the expression of the above four proteins. Briefly, we extracted the proteins by a cell total protein extraction kit (KeyGen-BioTECH, Nanjing, China) and determined their concentration. Then we mix the sample with the loading buffer and boil the mixture for 10 min. The proteins were then separated by PAGE, transferred to a polyvinylidene fluoride membrane, and sealed with 5% skimmed milk. After incubating with the primary antibody overnight at 4 °C, shake the membrane for 30 min and incubate with the secondary antibody (Beyotime, Shanghai, China,). Then, we rinse the membrane 3 times with Tris Buffered Saline with Tween 20, Finally, Bio-rad ChemiDoc Imaging system was applied to detect chemiluminescence.

GraphPad Prism 8 software (GraphPad, USA) was used to perform a one-way analysis of variance (ANOVA) to analyze the changes in the three sets of results. The data are expressed as mean ± standard deviation. The P-value < 0.05 (*) is considered statistically significant.

The tFNAs is a type of stable nucleic acid nanomaterial that is simple and efficient to synthesize, with no toxic side effects to the cell. The four strands of DNA in the tFNAs structure are of a specific sequence. Each single strand has three blocks of sequences, which are complementary to a block in another single-strand sequence [24]. Four single-stranded DNA (ssDNA) (Table 1) were used to obtain tFNAs (Fig. 1A). HPEC revealed that tFNAs were successfully synthesized from the single-stranded DNA (Fig. 1F). PAGE was used to prove that the molecular weight of tFNAs was 200 bp (Fig. 1B). AFM and TEM revealed the three-dimensional structure of the tFNAs (Figs. 1C and D) DLS was used to determine the particle size of the tFNAs (11.38 nm) and the electrostatic potential (−1.67 mV) (Fig. 1E).

In the field of bone tissue research, micro-CT can be used to quantify bone structure and bone density and can be used as an important basis for judging the stage of osteoporosis [25]. We established an OP model by removing both ovaries of the rat. The micro-CT showed the images of the femur metaphysis of control (sham operation) and OVX (model) rats 8 weeks after ovariectomy. As shown in Fig. 2A, compared with the control group, the trabecular bone of the OVX group was relatively sparse and the bone marrow cavity was significantly enlarged. Fig. 2B shows the number of Tb.N, Tb.Sp, and the SMI of the rats. Compared with the control group (sham operation), the trabecular bones of the model group changed from plate-shaped to rod-shaped, while the number decreased, and the degree of separation increased. The data

confirm that OP occurred in the OVX group, indicating that the OP-induction was successful.

DNA is a biological macromolecule with polyanionic properties that cannot pass through the plasma membrane to reach the cell. This property limits the effect of nucleic acid-based drugs. However, as a novel type of nucleic acid-based nanomaterial, tFNAs can reach the cell through caveolin-mediated endocytosis. Thus, tFNAs have good cell entry ability and elicit their own regulatory function in the cell [26]. To explore the uptake of tFNAs by OP-ASCs, the S1 chain was modified with Cy5 to synthesize tFNAs-Cy5, and then tFNAs-Cy5 and ssDNA were co-cultured with OP-ASCs for 24 h, respectively. The OP-ASCs were then placed under a confocal microscope to observe the intracellular uptake. Fig. 2C shows that ssDNA is hardly taken up by OP-ASCs, while tFNAs can be taken up by OP-ASCs after 24 h. Simultaneously, flow cytometry was used to detect the Cy5 fluorescence intensity in OP-ASCs. The fluorescence intensity of tFNAs was approximately 4 times that of ssDNA (Fig. 2D). The data prove that tFNAs can be effectively taken up by OP-ASCs and thus have a good ability to enter cells.

The function of stem cells is closely related to the ability of proliferation. In various stem cells such as ASCs, neural stem cells, and dental pulp stem cells, it was found that the proliferation ability of the cells was enhanced after tFNAs treatment [27]. Whether this function can still play a role in OP-ASCs is of great significance in our follow-up research. Therefore, we used different concentrations of tFNAs to treat OP-ASCs for 24 h to determine the effect of tFNAs on the cell viability of OP-ASCs. Based on the CCK8 asssay results (shown in Fig. 3D), different concentrations of tFNAs have different proliferation-promoting effects on the OP-ASCs. The concentration of 250 nmol/L had the strongest proliferation efficiency, which was significantly different from the control group. Therefore, the concentration of 250 nmol/L was chosen as the working concentration for subsequent experiments.

Cell migration is a complex cytological behavior regulated by multiple factors. It describes the action of cells in response to some signal factors that play a role in various biological processes such as wound healing, embryonic development, and the immune response [28]. After the establishment of *in vitro* scratch wound model, images of OP-ASCs migrating to the wound area were captured at 0 and 24 h (Fig. 3A). The OP-ASCs treated with 250 nmol/L tFNAs (tFNAs group) had a substantially higher migration distance than other group 24 h after scratches were made, *i.e.*, they exhibited the stronger migration ability than OP-ASCs group and ASCs group.

In order to detect the effect of tFNAs on the osteogenic ability of the OP-ASCs, we measured the ALP activity of each group on the 7th day of osteoblast differentiation, and the production of calcium nodules on the 21st day. ALP activity is an important marker of early osteoblast differentiation, and its expression is a very significant feature of osteoblast differentiation and maturation [29]. On day 7 of osteoblast differentiation, a BCIP/NBT alkaline phosphatase color reagent kit was used to determine the ALP activity. The ALP activity of the tFNAs group (OP-ASCs treated with 250 nmol/L tFNAs) was much higher than that of the OP-ASCs group (Fig. 3B). On the 21st day of osteoblast differentiation, the cells of each group were stained with Alizarin Red. The results show that the tFNAs group produced more calcium nodules than the OP-ASCs group (Fig. 4A). These results all indicate that tFNAs can promote the osteogenic differentiation of OP-ASCs.

RUNX2 is one of the Runt-related transcription factor family and is a transcription factor closely related to osteogenesis [30]. OCN is a non-collagenous protein abundant in the bones, most of which is tightly combined with the hydroxyapatite in the bone matrix. The gene expression of OCN is regulated by a variety of hormones, vitamins, and local cytokines. It is a specific product of osteoblasts and can reflect the activity of osteoblasts and the level

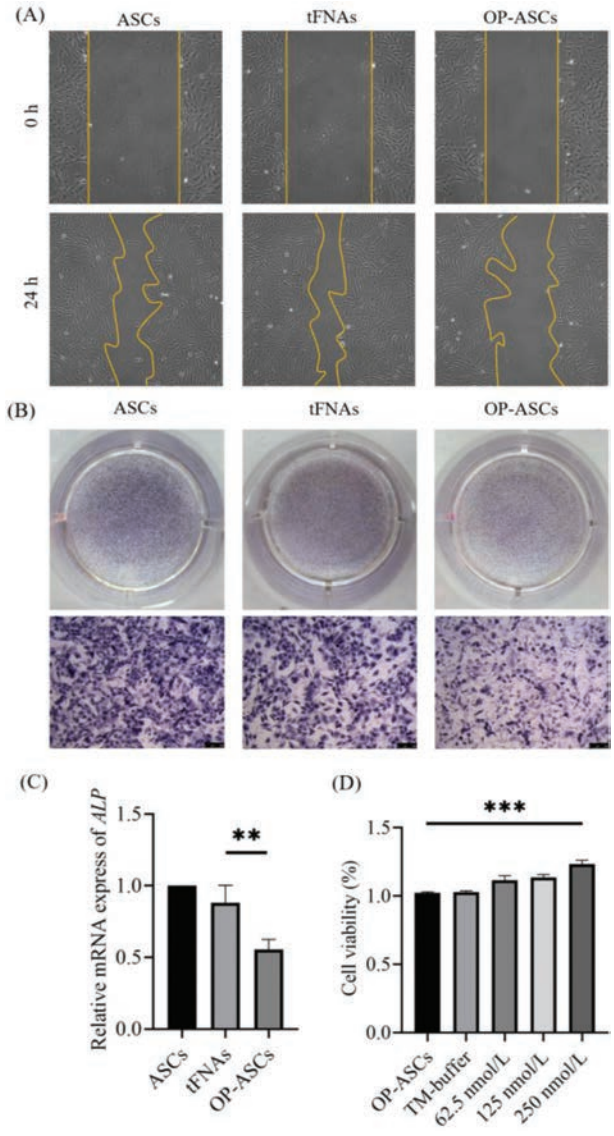

Fig. 3. The effect of tFNAs on the proliferation, migration and early osteogenesis of OP-ASCs (n = 3, $^{**}P < 0.01$, and $^{***}P < 0.001$). (A) *In vitro* scratch wound healing assay detected the effect of tFNAs with different concentrations on the migration of OP-ASCs. (B) Osteogenic differentiation was detected by ALP staining at day 7. (C) Gene expression level of *ALP* as detected by qPCR. (D) Cell viability in the OP-ASCs group and different tFNAs groups measured *via* the CCK-8 assay.

of bone metabolism conversion [31]. OPN is a negatively charged, non-collagenous glycoprotein in the bone matrix. OPN plays an important role in the mineralization and absorption of the bone matrix and is an important osteogenic phenotype determinant [32]. Exploring the protein and gene expression of *ALP, OCN, RUNX2* and *OPN* is an important means of examining and measuring the osteogenesis ability. Therefore, we first determined the expression of *OPN, OCN, ALP* and *RUNX2* genes in three groups of cells (OP-ASCs, tFNAs, and ASCs) by q-PCR. The expression of *OPN, OCN, ALP* and *RUNX2* genes in tFNAs group was significantly higher than that in the OP-ASCs group (Figs. 3C and 4E–G). Next, we applied western blot and immunofluorescence to investigate the protein expression of OPN, OCN, ALP and RUNX2 in the three groups of cells. The results of the western blots and immunofluorescence showed that the protein expressions of OPN, OCN, ALP and RUNX2 in the tFNAs group were also higher than those of the other two groups (Figs. 4B–D).

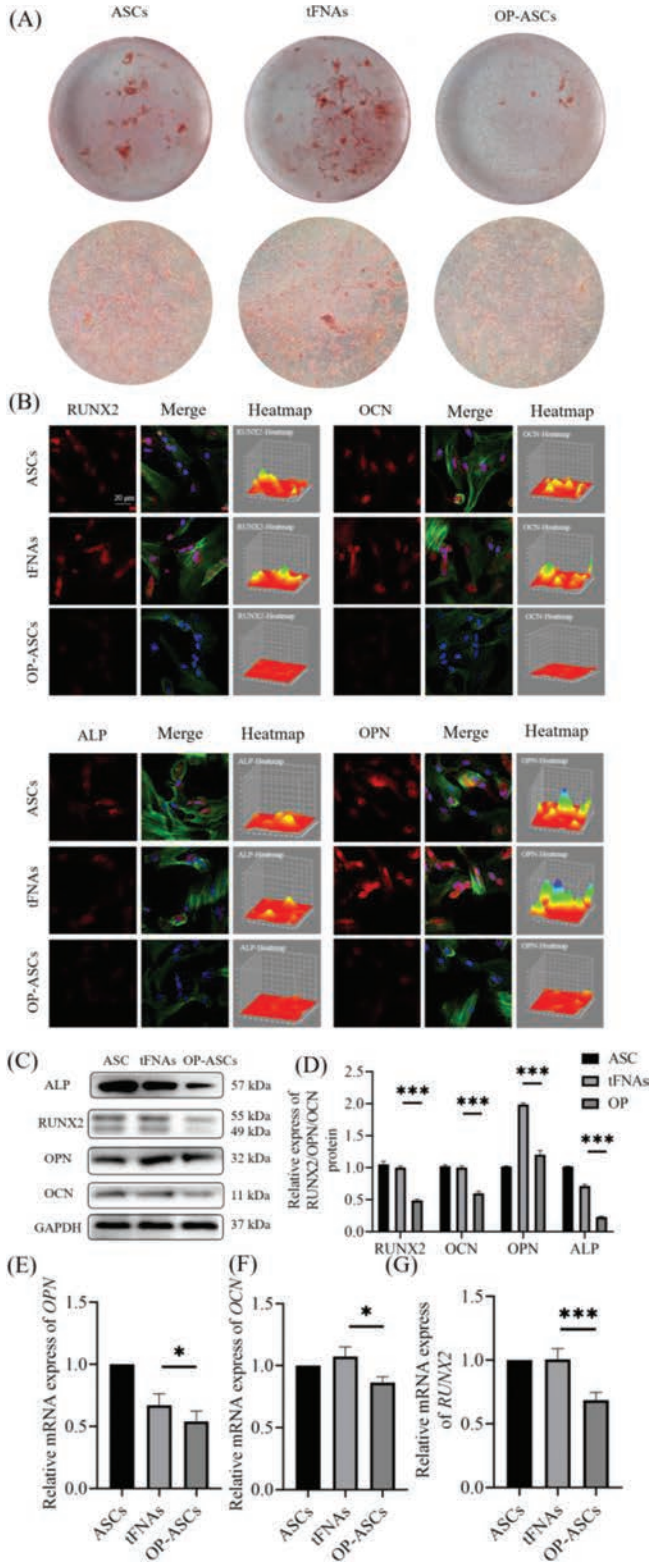

Fig. 4.. Effect of tFNAs on osteogenic differentiation of OP-ASCs ($n = 3$, $^{*}P < 0.05$, and $^{***}P < 0.001$). (A) *In vitro* scratch wound healing assay detected the effect of tFNAs with different concentrations on the migration of OP-ASCs. (B) Immunofluorescence detection of RUNX2, OPN, OCN and ALP expression (nucleus: blue; cytoskeleton: green; and target protein: red). Scale bars are 20 μm. (C) Gene expression level of *ALP* as detected by qPCR. (D) Cell viability in the OP-ASCs group and different tFNAs groups measured *via* the CCK-8 assay.

In summary, this study successfully synthesized a new type of nanomaterial tFNAs, which has a good ability to enter OP-ASCs and can promote the proliferation and migration of OP-ASCs. Except that tFNAs can also promote the protein and gene expression of *OPN, RUNX2, OCN, ALP*, and restore the osteogenic potential of OP-ASCs, and play an important regulatory role in OP's autologous stem cell transplantation therapy. Therefore, tFNAs is a promising, safe and effective nanomaterial for the treatment of OP.

Declaration of competing interest

The authors declare that they have no known competing financial interests or personal relationships that could have appeared to influence the work reported in this paper.

Acknowledgments

This study was supported by the National Key R&D Program of China (No. 2019YFA0110600), National Natural Science Foundation of China (Nos. 82171006, 81970986, 81771125, 82001432), China Postdoctoral Science Foundation (Nos. 2020TQ0213, 2020M683319), and West China Hospital Postdoctoral Science Foundation (No. 2020HXBH104).

References

[1] S. Das, J.C. Crockett, Drug Des. Devel. Ther. 7 (2013) 435–448.
[2] L.G. Raisz, J. Clin. Invest. 115 (2005) 3318–3325.
[3] S. Amin, S.J. Achenbach, E.J. Atkinson, S. Khosla, L.J. Melton, J. Bone Miner. Res. 29 (2014) 581–589.
[4] S.R. Cummings, L.J. Melton, Lancet 359 (2002) 1761–1767.
[5] D.M. Black, C.J. Rosen, N. Engl. J. Med. 374 (2016) 254–262.
[6] S. Li, Y. Liu, T. Tian, et al., Small 17 (2021) 2104359.
[7] K. Huang, G. Liu, Z. Gu, J. Wu, Chin. Chem. Lett. 31 (2020) 3190–3194.
[8] Q. Yuan, J. Huang, C. Xian, J. Wu, ACS Appl. Mater. Inter. 13 (2021) 2165–2178.
[9] S. Khosla, L.C. Hofbauer, Lancet Diabetes Endo. 5 (2017) 898–907.
[10] F. Cosman, D.B. Crittenden, J.D. Adachi, et al., N. Engl. J. Med. 375 (2016) 1532–1543.
[11] S. Verma, J.H. Rajaratnam, J. Denton, J.A. Hoyland, R.J. Byers, J. Clin. Pathol. 55 (2002) 693–698.
[12] H. Mizuno, M. Tobita, A.C. Uysal, Stem Cells 30 (2012) 804–810.
[13] L. Wang, C. Huang, Q. Li, et al., Cell Prolif. 50 (2017) e12328.
[14] T. Zhang, T. Tian, Y. Lin, Adv. Mater. (2021), doi:10.1002/adma.202107820.
[15] T. Zhang, T. Tian, R. Zhou, et al., Nat. Protoc. 15 (2020) 2728–2757.
[16] W. Ma, Y. Zhan, Y. Zhang, et al., Signal Transduct. Target. Ther. 6 (2021) 351.
[17] S. Sirong, C. Yang, T. Taoran, et al., Bone Res. 8 (2020) 6.
[18] W. Cui, X. Yang, X. Chen, et al., Adv. Funct. Mater. 31 (2021) 2105152.
[19] J. Li, L. Xiao, N. Yan, et al., Adv. Funct. Mater. 31 (2021) 2104141.
[20] M. Zhang, X. Zhang, T. Tian, et al., Bioact. Mater. 8 (2022) 368–380.
[21] W. Fu, L. Ma, Y. Ju, et al., Adv. Funct. Mater. 31 (2021) 2101435.
[22] Y. Sun, Y. Liu, B. Zhang, et al., Bioact. Mater. 6 (2021) 2281–2290.
[23] Y. Li, R. Zhou, D. Xiao, et al., Chem. Eng. J. 403 (2021) 126344.
[24] T. Zhang, W. Cui, T. Tian, S. Shi, Y. Lin, ACS Appl. Mater. Interfaces 12 (2020) 47115–47126.
[25] E.L. Ritman, Annu. Rev. Biomed. Eng. 13 (2011) 531–552.
[26] J. Li, H. Pei, B. Zhu, et al., ACS Nano 5 (2011) 8783–8789.
[27] S. Li, T. Tian, T. Zhang, X. Cai, Y. Lin, Mater. Today 24 (2019) 57–68.
[28] S. Modi, S.M. Goswami, G.D. Gupta, S. Mayor, Y. Krishnan, Nat. Nanotechnol. 4 (2009) 325–330.
[29] Y. Li, L. Wang, M. Zhang, et al., Cell Prolif. 53 (2020) e12834.
[30] T. Komori, Histochem. Cell Biol. 149 (2018) 313–323.
[31] S.C. Moser, B.C.J. van der Eerden, Front. Endocrinol. 9 (2019) 794.
[32] M.A. Icer, M. Gezmen-Karadag, Clin. Biochem. 59 (2018) 17–24.